RSC Advances

PAPER

View Article Online
View Journal | View Issue

Cite this: *RSC Adv.*, 2022, **12**, 35779

New amino acid propyl ester ibuprofenates from synthesis to use in drug delivery systems†

Paula Ossowicz-Rupniewska, *[a] Kaja Szczepkowska,[a] Paulina Bednarczyk,[a] Małgorzata Nowak,[a] Anna Nowak,[b] Wiktoria Duchnik,[b] Łukasz Kucharski,[b] Łukasz Struk,[c] Adam Klimowicz [b] and Zbigniew Czech [a]

Received 14th September 2022
Accepted 29th November 2022

DOI: 10.1039/d2ra05804a

rsc.li/rsc-advances

This study aimed to evaluate the effect of introducing structural modification of ibuprofen in the form of an ion pair on the permeability of ibuprofen through the skin and the properties of the adhesive layer of the medical patch produced. The active substances tested were the salts of ibuprofen obtained by pairing the anion of ibuprofen with organic cations such as propyl esters of amino acids such as tyrosine, tryptophan, histidine, or phenylalanine. For comparison, the penetration of unmodified ibuprofen and commercially available patches was also tested. Acrylate copolymers based on isobornyl methacrylate as a biocomponent and a monomer increasing the T_g ("hard") were used to produce the adhesive layer of transdermal patches. The obtained patches were characterized in terms of adhesive properties and tested for the permeability of the active ingredient and the permeability of the active ingredient through the skin. This study demonstrates the possibility of developing acrylic-based photoreactive transdermal patches that contain biocomponents that can deliver a therapeutically appropriate dose of ibuprofen.

Introduction

According to the International Association for the Study of Pain (IASP), pain is a subjectively unpleasant and negative sensory and emotional impression arising from (so-called nociceptive) stimuli that damage or threaten the tissue. Pain is a subjective feeling, so whatever the patient calls it, regardless of its objective symptoms.[1–4] Pain is a serious health problem, even a disease. Therefore, pain management is extremely important from the point of view of the patient's comfort of life and health. Pain treatment is carried out according to the analgesic ladder, *i.e.*, using painkillers and other pharmaceuticals to reduce the patient's pain sensations. This scheme distinguishes three levels of interactivity of treatment, depending on the level of pain perception.[5] Non-steroidal anti-inflammatory drugs are at the root of the analgetic ladder and are used alongside paracetamol as the first choice for pain management. They are mainly used for mild pain relief (1–4 on the numerical scale-NRS).[5,6]

Various routes of drug administration are used to treat pain, including drug delivery through the skin. Topical and transdermal application of drugs is one of the most important methods of delivering them to the body.[7] It is known that the transdermal administration of a drug to induce a systemic effect has several significant advantages and, in many situations, is an advantage over the administration of oral or intravenous drugs. Among the many advantages of transdermal administration of the drug, the possibility of avoiding the first-pass effect (hepatic metabolism) and the elimination of side effects of the drug on the gastrointestinal tract deserves special attention. In addition, attention should be paid to the elimination of the possible decomposition of the active substance in the gastrointestinal tract as well as the exclusion of the possibility of drug interactions with food and other orally administered drugs. Furthermore, the use of this route of administration allows for obtaining the desired therapeutic effect after the absorption of lower doses. The appropriate modification with increased permeability through biological membranes can significantly reduce these doses. In this case, the drug substance's absorption rate depends on its release rate, a property that can be appropriately controlled depending on the desired effect. In addition, administration through the skin reduces the frequency of drug application with a short biological half-life, which is especially important in treating chronic diseases.[7–9]

For this route of drug administration, a very important factor in limiting penetration is the skin barrier which reduces the penetration efficiency and limits the absorption of the compounds. This layer is the greatest obstacle to the transport

[a]*Department of Chemical Organic Technology and Polymeric Materials, Faculty of Chemical Technology and Engineering, West Pomeranian University of Technology, Piastów Ave. 42, Szczecin 71-065, Poland. E-mail: possowicz@zut.edu.pl*

[b]*Department of Cosmetic and Pharmaceutical Chemistry, Pomeranian Medical University in Szczecin, Powstańców Wielkopolskich Ave. 72, Szczecin 70-111, Poland*

[c]*Department of Organic and Physical Chemistry, Faculty of Chemical Technology and Engineering, West Pomeranian University of Technology, Piastów Ave. 42, Szczecin 71-065, Poland*

† Electronic supplementary information (ESI) available. See DOI: https://doi.org/10.1039/d2ra05804a

of active substances and is considered the primary barrier to the permeation of molecules. It is mainly composed of lipid substances such as ceramides, cholesterol, fatty acids, cholesterol esters, and small amounts of phospholipids.[10] Among the available and topically applied drugs, a significantly small group can passively cross the skin barrier in amounts sufficient to obtain a therapeutic effect.[11] This route of administration is used to reduce unwanted side effects, avoid first-pass metabolism in the liver, and minimize gastrointestinal side effects.[12] However, due to the poor penetration capacity through the stratum corneum, it is difficult to obtain its effective concentration.[13]

One of the most popular painkillers is ibuprofen, which is used in various pharmaceutical formulations, including those administered through the skin.[14] However, ibuprofen is characterized by relatively low solubility in water, especially in an acidic environment. The consequence of this property is the relatively slow pharmacological action of ibuprofen.[15–19] In addition, ibuprofen has a very low skin permeability. Therefore, research is currently being conducted to obtain its derivatives with similar pharmaceutical activity, with increased solubility and permeability through the skin, and thus – substances with a faster therapeutic effect. In order to increase the solubility of ibuprofen and its bioavailability, various types of structural modifications of the compound are used. The first and most basic modification of ibuprofen is to convert the compound into a salt form. The mechanism of this modification is relatively simple – it consists in replacing an acid proton with a salt cation. Ibuprofen salts can be of organic and inorganic origin, for example, sodium, potassium, calcium, diethylamine, tris(hydroxymethyl)aminomethane, and tetraethylammonium.[20–26] Many strategies for modifying ibuprofen, such as modifying the particle size, and using solvents or surfactants, failed to achieve the intended results, or the modification costs significantly exceeded the production costs of ibuprofen. The least complicated and most effective option remained ibuprofen salt formation.[15,27] An attractive solution to the solubility problem is forming ibuprofen salt with amino acids. Previous studies have shown that using basic amino acids, such as lysine or arginine, not only increases the solubility of ibuprofenate but also does not change the action or effectiveness of the active substance.[28] In addition, attention was paid to using amino acids. Compared to their inorganic counterparts, they are characterized by lower basicity in the formulation and self-buffering effect.[29] Subsequent studies have shown that using amino acids reduces the risk of the common ion effect in the stomach's acidic environment.[30] In addition to the advantages mentioned above, using arginine salts reduces the risk of complications in the cardiovascular system due to the use of NSAIDs.[31] Another advantage is the production of pleasant-tasting salts. Additionally, the drug's action can be enriched with the action of amino acids.[28] An interesting alternative is using a salt – an amino acid ester as the cation. Compounds of this type are formed due to the combination of ibuprofen, which acts as an anion, and an L-amino acid ester. The researchers' reports on the work on these compounds indicate that this type of modification of ibuprofen allows to "design" of the properties of the resulting salt, thanks to the selection of individual reagents.[15,32,33] Furukawa *et al.* obtained an amino acid ionic liquid based on L-proline ethyl ester. It has been shown that the obtained compound shows increased permeability after 48 h of testing and toxicity comparable to the proline ethyl ester.[34] Our previous publications refer to the salts – ibuprofenates of L-valine alkyl esters. As a result of the work, derivatives with different alkyl chain lengths from C2–C6 and with different branching were obtained. The research carried out by our team has shown that these compounds act as promoters of the penetration of the active substance through the skin. It has been shown that the use of the ibuprofen mentioned above salts has a particular application in the local treatment of pain and significantly increases the bioavailability of the active substance in the transdermal administration of the drug. And the use of this modification of ibuprofen brings additional advantages and may be a source of exogenous amino acids. In our publications, we have shown that using the C3 alkyl chain is most advantageous.[15,35] As part of subsequent studies, we obtained derivatives of isopropyl alcohol using various types of amino acids.[33] Unfortunately, due to the use of a secondary alcohol, it was impossible to perform syntheses using amino acids with an aromatic (tyrosine, tryptophan) or a heterocyclic side chain (histidine).

This publication presents the synthesis of four new compounds – L-amino acid propyl esters (Tyr, Trp, His, Phe). We fully characterize them, compare their properties, and present their use as active compounds in transdermal patches with a biomonomer-based adhesive developed by our team.

Results and discussion

Active compounds – ibuprofen derivatives

As a result, four ibuprofenates of amino acid propyl esters were obtained, such as phenylalanine [PheOiPr][IBU],[36] histidine [HisOiPr][IBU], tyrosine [TyrOiPr][IBU] and tryptophan [TrpOiPr][IBU], of which the last three were obtained for the first time. All compounds obtained were identified based on ^{1}H and ^{13}C NMR, ATR-FTIR, and elemental analysis. NMR spectra and elemental analysis results confirmed purity. All ^{1}H and ^{13}C NMR, FTIR spectra, TG and DSC curves, and XRD patterns for [AAOPr][IBU] are available in ESI (S1–S25†).

For complete identification – NMR, FT-IR spectra assignments, and elemental analysis, see the Experimental section.

The ionic structure of the compounds obtained was confirmed based on the analysis of ^{1}H, ^{13}C NMR, and FTIR spectra. Fig. 1 presents a summary of the ^{1}H NMR spectra of the obtained ibuprofenates. The figure shows the signal from the protonated amino group of the amino acid. The NH_3^+ signal shift values range from 8.37 ppm (for the [HisOPr][IBU]) to 4.77 ppm (for the [PheOPr][IBU]). The integration of this signal proves the protonation of the amino group. The greatest revealing effect was observed for [HisOPr][IBU], possibly due to two ibuprofenate anions in the molecule.

Another evidence of obtaining the ionic structure is changing chemical shifts in the ^{13}C NMR spectrum. Fig. 2 summarizes the ^{13}C NMR spectra of the obtained ibuprofen

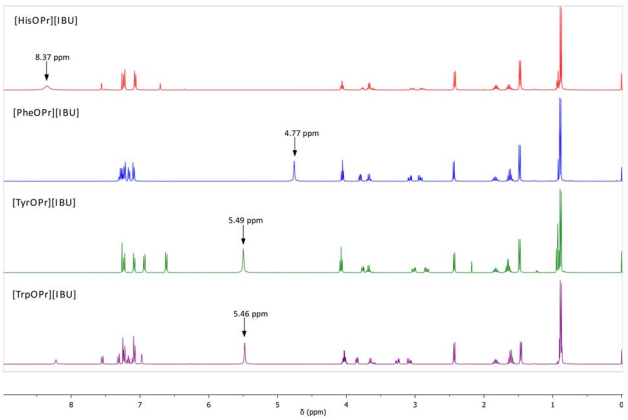

Fig. 1 ^{1}H NMR spectra of obtained amino acid propyl ester ibuprofenates, from the top: [HisOPr][IBU] (red), [PheOPr][IBU] (blue), [TyrOPr][IBU] (green), [TrpOPr][IBU] (purple). The arrow marks the signal from the NH_3^+ group of the amino acid.

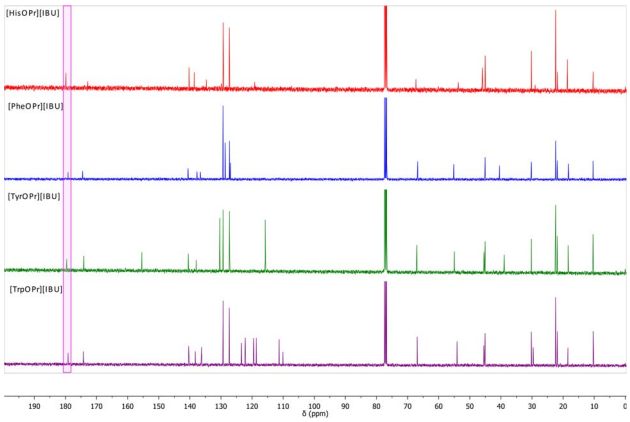

Fig. 2 ^{13}C NMR spectra of obtained amino acid propyl ester ibuprofenates, from the top: [HisOPr][IBU] (red), [PheOPr][IBU] (blue), [TyrOPr][IBU] (green), [TrpOPr][IBU] (purple). Carbonyl carbons from ibuprofen anions are marked in a pink square.

salts. The signal from the carbonyl group in ibuprofen is 181.16 ppm,[15,37–39] while in the case of obtaining the salt of ibuprofen esters, this signal is shifted towards the lower values – from 1.29 ppm (for [HisOPr][IBU]) to 2.02 ppm (for [TrpOPr][IBU]).

The presence of two characteristic absorption bands – asymmetric $\nu(COO^-)_{as}$ and symmetric stretching vibrations $\nu(COO^-)_{sym}$ was noted in the ATR-FTIR spectra, which once again confirm the ionic structure of the compounds obtained.[40] The difference above 200 cm^{-1} between the frequency values of these two bands confirmed the presence of the carboxylate anion COO^- and the ionic structure of ibuprofenates. Fig. 3 shows the ATR-FTIR spectra of the compounds obtained, and the characteristic vibrations are marked.

An XRD analysis was performed to confirm the crystallinity of the obtained compounds. Fig. 4 summarizes the XRD patterns of ibuprofen and amino acid propyl ester ibuprofenates. It has been shown that the diffractograms of the obtained

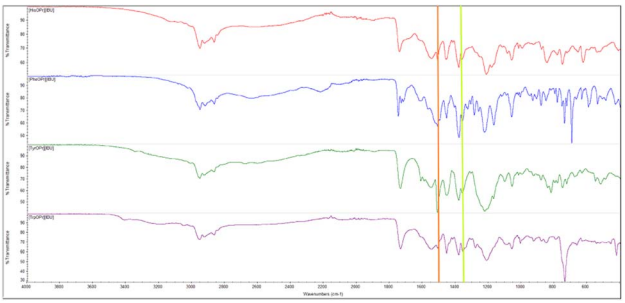

Fig. 3 ATR-FTIR spectra of obtained amino acid propyl ester ibuprofenates, from the top: [HisOPr][IBU] (red), [PheOPr][IBU] (blue), [TyrOPr][IBU] (green), [TrpOPr][IBU] (purple). $\nu(COO^-)_{sym}$ and $\nu(COO^-)_{as}$ stretching vibrations marked in orange and lime, respectively.

salts differ from that of the unmodified ibuprofen, while for ibuprofen, the diffractogram is consistent with the reference diffractogram (PDF 96-230-0213).

The physicochemical properties, such as melting point, crystallization temperature, thermal stability, and specific rotation, were determined for all obtained compounds. Table 1 summarises the results.

Based on thermogravimetric studies, the stability of the tested L-amino acid ibuprofenates was assessed. All TG, dTG, and c-DTA curves are in the ESI (Fig. S14–17†). A different number of degrees of degradation was observed, depending on the amino acid used in the synthesis. [PheOPr][IBU] decomposed into two stages, while [TrpOPr][IBU] decomposed into four steps. The remaining compounds unfolded in three stages. Among the tested compounds, the least stable was [TyrOPr][IBU], and the largest – [TrpOPr][IBU], which was more stable than unmodified ibuprofen. The melting points of [PheOPr][IBU] and [TrpOPr][IBU] do not exceed 100 °C. This and the confirmed ionic structure (based on the analysis of NMR and

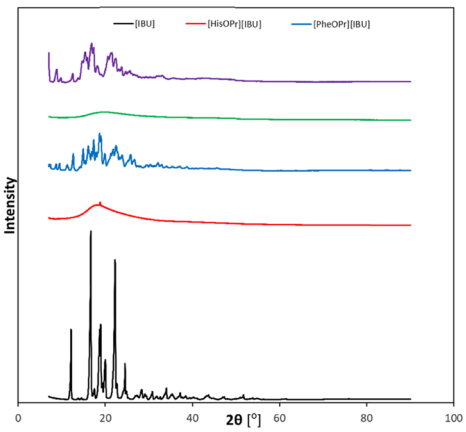

Fig. 4 X-ray diffraction patterns of ibuprofen and obtained amino acid propyl ester ibuprofenates, from the top: [TrpOPr][IBU] (purple), [TyrOPr][IBU] (green), [PheOPr][IBU] (blue), [HisOPr][IBU] (red), [IBU] (black).

Table 1 Parameters characterizing thermal stability and phase transitions of L-amino acid propyl esters ibuprofenates[a]

No.	Compound	Colour and state	T_m/°C	T_c/°C	T_{onset}/°C	T_{max}/°C	$[\alpha]_\lambda^{20}$
1	[IBU][b]	White solid	78.6	—	189.8	218.7	—
2	[HisOPr][IBU]	Brownish solid	—	—	157.5	212.5	−0.7
3	[PheOPr][IBU][c]	White solid	81.4	54.0	157.0	210.4	+14.9
4	[TyrOPr][IBU]	Yellowish wax	—	—	148.1	209.4	+1.8
5	[TrpOPr][IBU]	Orange wax	59.6	—	269.3	219.3	+8.9

[a] T_c – cold crystallization temperature; T_m – melting point; T_{onset} – the onset of the thermal degradation; T_{max} – maximum decomposition temperature; $[\alpha]_\lambda^{20}$ – specific rotation. [b] Data for these compounds were earlier reported in ref. 33. [c] Data for these compounds were earlier reported in ref. 36.

FT-IR spectra) allow classifying these compounds into the group of ionic liquids.

Since optically active amino acids were used for the syntheses, the optical rotation of the obtained derivatives was also examined (Table 1). All the derivatives obtained show the ability to rotate the plane of polarized light. All the obtained ibuprofenates, except [HisOPr][IBU], show the direction of rotation of the plane of light polarized consistent with the starting amino acids. In the case of [HisOPr][IBU], there was a change in the direction of turning the plane of left-polarized light.

To properly classify the obtained ibuprofen derivatives, their solubility in water and organic solvents was examined, and the obtained results are presented in Table 2. All L-amino acid propyl ester ibuprofenates were soluble in ethanol, dimethyl sulfoxide, methylene chloride, and chloroform. It can be seen that the use of amino acids such as histidine, tyrosine, or tryptophan affects the solubility in non-polar solvents such as *n*-hexane.

The water solubility of drugs is used to assess their bioavailability and efficacy. Therefore this parameter is key in the evaluation of potential new drugs. An equally important parameter is the partition coefficient, which predicts drug hydrophobicity and partitioning in biological systems. The solubility parameter in water and *n*-octanol–water partition coefficient was determined, and the results were summarised in Table 3. Converting the drug into an amino acid propyl ester salt form is a very good modification of the drug in order to improve its properties. Thanks to this, there was a clear increase in the solubility of the obtained derivatives compared to ibuprofen by about 60 times (based on the concentration of the active substance). The highest solubility in water was obtained for [HisOPr][IBU] (4.775 ± 0.046 g IBU per dm^3), while [TyrOPr][IBU] had the lowest (4.188 ± 0.065 g IBU per dm^3). The differences in solubilities for the derivatives obtained were insignificant.

The structural change greatly influenced the lipophilicity of the obtained derivatives. All obtained ibuprofen and amino acid isopropyl ester ibuprofenates showed a positive log *P*, but they were lower than ibuprofen. All the salts obtained are, therefore, more hydrophilic. The distribution coefficient of the obtained compounds was similar and amounted to about +1. The lipophilicity of the obtained salts was ranked in ascending order: [HisOPr][IBU] < [PheOPr][IBU] < [TrpOPr][IBU] < [TyrOPr][IBU].

Finally, studies *in vitro* on the permeability of the active substance through pig skin were also carried out. Permeation profiles for ibuprofen and amino acid propyl ester ibuprofenates are plotted in Fig. 5. The cumulative mass of the individual compounds, determined after 24 h of permeation, was as follows: [PheOPr][IBU] > [HisOPr][IBU] > [TrpOPr][IBU] > [TyrOPr][IBU] and [IBU]. The permeation of all ibuprofen derivatives in the acceptor phase during 24 h of the study was significantly higher than free ibuprofen. After 24 h of permeation, the cumulative mass of penetrated compound was about ten times higher for the obtained derivatives than for ibuprofen. [PheOPr][IBU] was characterized by the most statistically significantly increased cumulative mass, and the cumulative amount of substance permeated during the 24 h study was 454.86 μg cm^{-2} (Table 4, Fig. 5 and S26†). However, no significant differences were found between the penetration of other

Table 2 Solubility of ibuprofen and amino acid propyl ester ibuprofenates in organic solvents at room temperature[a]

No.	Solvent	[IBU][33]	[HisOPr][IBU]	[PheOPr][IBU]	[TyrOPr][IBU]	[TrpOPr][IBU]
1	EtOH (51.9)	+	+	+	+	+
2	DMSO (45.1)	+	+	+	+	+
3	CH_2Cl_2 (40.7)	+	+	+	+	+
4	$CHCl_3$ (39.1)	+	+	+	+	+
5	ETA (38.1)	+	+	+	+	+
6	Et_2O (34.5)	+	−	−	−	−
7	Toluene (33.9)	+	±	−	−	−
8	*n*-Hexane (31.0)	−	+	−	+	+

[a] Solvents were ranked with decreasing values of empirical solvent polarity parameters, $E_T(30)$[41] ("+": soluble >100 mg cm^{-3}; "±": partially soluble 33–100 mg cm^{-3}; "−": insoluble <33 mg cm^{-3}) at the room temperature by modified Vogel's method.[42]

Table 3 The solubility and *n*-octanol–water partition coefficient (log *P*) of ibuprofen and amino acid propyl ester ibuprofenates

No.	Compound	Solubility in water		log *P*
		g dm^{-3}	g IBU per dm^3	
1	[IBU][33]	0.076 ± 0.001	0.076 ± 0.001	+3.208
2	[HisOPr][IBU]	9.801 ± 0.067	4.775 ± 0.046	+0.963
3	[PheOiPr][IBU]	9.481 ± 0.066	4.596 ± 0.161	+1.021
4	[TyrOPr][IBU]	8.569 ± 0.022	4.188 ± 0.065	+1.055
5	[TrpOPr][IBU]	9.396 ± 0.027	4.577 ± 0.037	+1.044

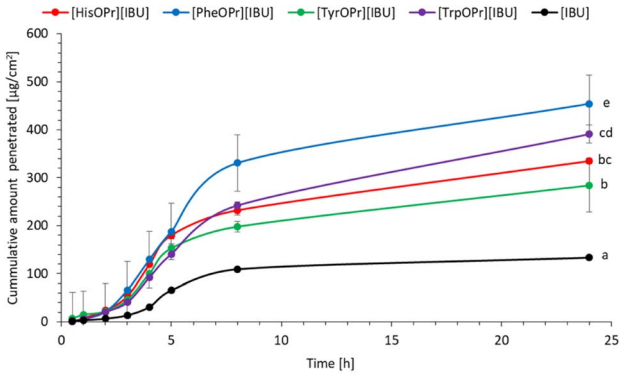

Fig. 5 Ibuprofen and amino acid propyl ester ibuprofenates permeation profiles. Values are the means with standard deviation; $n = 3$.

derivatives, *i.e.*, [HisOPr][IBU], [TyrOPr][IBU], and [TrpOPr][IBU]. The cluster analysis test also confirms these results, in which, *i.e.*, [HisOPr][IBU], [TyrOPr][IBU], and [TrpOPr][IBU] form a separate cluster (Fig. S27†). The similarity between all compounds was also found using the Wilcoxon test, which showed a statistically significant difference between all derivatives and pure ibuprofen ($p < 0.05$) (Table S1†).

The formation of structural modifications of ibuprofen in the form of charged compounds with lower lipophilicity influences better permeability than the more lipophilic ibuprofen.

Based on the *in vitro* penetration efficiency studies for ibuprofen and its derivatives, the following permeation parameters were determined: flux (J_{SS}, μg IBU per cm^2 h), apparent permeability coefficient ($K_P \times 10^3$, cm h^{-1}), lag time (L_T, h), diffusion coefficient in the skin ($D \times 10^4$, cm^2 h^{-1}), skin partition coefficient (K_m), and percent drug permeated after 24 h (Q). The permeability parameters of the obtained compounds were similar to those determined for ibuprofen. The steady-state flux of the [AAOPr][IBU] from ethanol solution was from 21.33 μg IBU per cm^2 for [HisOPr][IBU], to 28.01 for [PheOPr][IBU], while for ibuprofen – 25.87 μg IBU per cm^2 h, respectively. In the case of using ibuprofenates, higher flows of active substances were obtained, which can be useful in formulations administered through the skin, like transdermal patches. The permeability coefficient, a quantitative measure of the rate at which a molecule can cross the skin, was also determined. This parameter comprises factors related to the drug, the barrier and their interaction. Furthermore, it eliminates the effect of concentration. K_P values for obtained compounds ranged from 14.918 (for [HisOPr][IBU]) to 19.606 cm h^{-1} (for [PheOPr][IBU]). The lag time depending on the derivatives was shorter than the unmodified ibuprofen. The diffusion coefficient in the skin was similar for the obtained salts than for IBU. The skin partition coefficient, as the equilibrium solubility of the drug in the stratum corneum concerning its solubility in the vehicle, was also determined. Its values were generally lower than for ibuprofen (0.281). They ranged from 0.192 to 0.229 for [HisOPr][IBU] and [TyrOPr][IBU], respectively. Moreover, it was shown that the percentage of the applied dose after 24 h (in terms of ibuprofen) was higher for [TrpOPr][IBU] and [PheOPr][IBU]. The obtained results suggest that the obtained compounds may promote skin permeability, and the choice of the applied structural modification should be decided based on factors such as molar mass, solubility, or lipophilicity.

Fig. 6 shows the results of the permeation rate of the compounds obtained. It is clearly visible that the rates for the derivatives obtained are higher than for ibuprofen. The highest permeation rate generally was observed between 3–5 h.

Interestingly, in the case of the derivatives obtained, much larger doses penetrate at the beginning of the study, which may help to obtain a faster therapeutic effect science fast, and increased permeation causes a quicker decrease in inflammation in the underlying tissues.[43]

After the permeability study was completed, accumulation in the skin was also determined. Fig. 7 presents the mass of [IBU] and its amino acid propyl salts accumulated in porcine skin after 24 h of penetration. All the compounds used accumulated in the skin to a lesser extent than ibuprofen. The accumulation in the skin of the obtained derivatives was similar and ranged from 461.56 ± 29.77 for [HisOPr][IBU], 595.41 ± 76.32 for

Table 4 The solubility and *n*-octanol–water partition coefficient (log *P*) of ibuprofen and amino acid propyl ester ibuprofenates[a]

No.	Compound	CUM	J_{SS}	K_P	L_T	D	K_m	Q
1	[IBU]	133.35	25.87	18.110	2.582	32.272	0.281	9.33
2	[HisOPr][IBU]	335.13	21.33	14.918	2.141	38.914	0.192	7.90
3	[PheOPr][IBU]	454.86	28.01	19.606	1.705	48.863	0.200	15.80
4	[TyrOPr][IBU]	284.27	25.57	17.898	2.133	39.068	0.229	9.51
5	[TrpOPr][IBU]	319.22	22.72	15.907	2.179	38.247	0.208	12.42

[a] CUM – cumulative permeation mass (μg cm^{-2}); J_{SS} – steady-state flux (μg cm^{-2}); K_P – permeability coefficient (cm h^{-1}); L_T – lag time (min); D – diffusion coefficient (cm^2 h^{-1}); K_m – skin partition coefficient; Q – the percentage of the applied dose after 24 h.

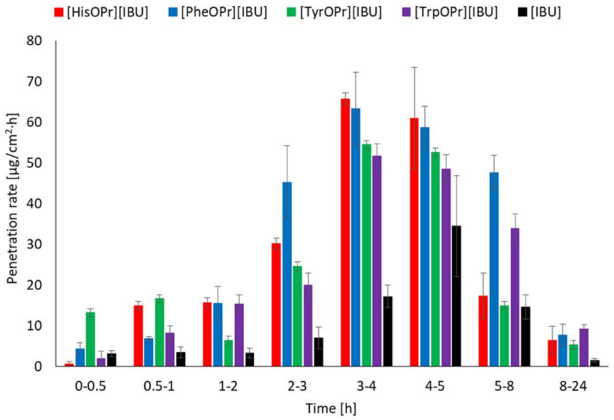

Fig. 6 The permeation rate of ibuprofen and amino acid propyl ester ibuprofenates during the 24 h permeation; $\alpha = 0.05$ (mean ± SD, $n = 3$).

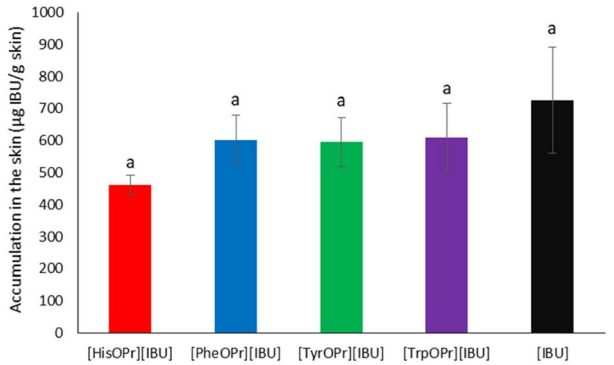

Fig. 7 Ibuprofen and amino acid propyl ester ibuprofenates permeation profiles. Values are the means with standard deviation; $n = 3$.

[TrpOPr][IBU], 602.86 ± 76.98 for [PheOPr][IBU], to 609.35 ± 106.07 μg IBU per g skin for [TyrOPr][IBU]. While for the [IBU], it was 725.49 ± 164.6184 μg IBU per g skin.

The use of active ibuprofen derivatives in transdermal patches

Synthesis of the acrylic pressure-sensitive adhesives (PSA). Our previous report showed that a transdermal drug delivery system could be developed as an adhesive patch based on photoreactive acrylate copolymers with new acrylic-based PSA with a biocomponent. Previous studies have shown that unmodified ibuprofen can be easily released from the prepared patches and penetrate pig skin membranes. In addition, a relatively consistent release of IBU was observed, which may benefit the design of transdermal patches containing drugs requiring sustained-release kinetics. Criteria such as the type of raw material, available technologies, and application form the basis of trends in developing adhesives for medical devices.[44]

Therefore, based on our previous research, the PSA containing 5 wt% of acrylic acid, 70 wt% 2-hydroxyethyl acrylate, and 25 wt% isobornyl methacrylate was selected for the preparation of the transdermal patches due to its optimal parameters (viscosity, solids content).

Preparation of transdermal patches (TP). The pressure-sensitive adhesive (PSA) employed consists of an acrylate copolymer consisting of acrylic acid, 2-hydroxyethyl acrylate, and isobornyl methacrylate was used to obtain a transdermal patch. The active substance was introduced into the polymer matrix before the cross-linking process. Ibuprofen, sodium ibuprofenate and [PheOPr][IBU], [TyrOPr][IBU], and [Trp][IBU] were used in the research. The content of the active substance in the adhesive was calculated based on the previously performed characteristics of the adhesive: the molar mass of the compounds used and the solids content of the adhesive. The active substance content was assumed based on available commercial products, *i.e.*, 200 mg of active substance per 140 cm^2 of the adhesive surface. The thus obtained adhesive compositions were coated with a layer with a thickness of 250 μm using a semi-automatic coater on a polyester film. The obtained films were then dried and cross-linked with a UV lamp. At the end of the process, the obtained films were covered with siliconized paper. FTIR spectra of obtained patches are available in ESI (S28–S33†).

Characteristics of transdermal patches. The obtained transdermal patches without and with active substances were examined in terms of thermal stability, phase transition temperatures, cohesion, adhesion, and tack. The results are presented in Table 5.

It was shown that the addition of the active substance influences the glass transition temperature of the obtained adhesive films. The glass transition temperature of the adhesive film without the addition of active substance is −19.80 °C. For patches with the addition of IBU, [PheOPr][IBU], and [TyrOPr][IBU], the glass transition temperature obtained was lower than the glass transition temperature of the patch without the addition of the active ingredient. The addition of [IBU][Na] and [TrpOPr][IBU] slightly increases the glass transition temperature of the patch. All DSC curves are included in the ESI (Fig. S40–45†).

The thermal stability of the obtained patches was tested using thermogravimetric analysis. The following parameters were determined: onset decomposition temperature and temperature corresponding to the weight loss of 50% (determined from TG curves) and maximum decomposition temperatures (determined from DTG curves). These properties were summarized in Table 5 and Fig. S34–39 (ESI†). Among the tested polyacrylate compositions, the highest stability was characteristic for an adhesive containing sodium ibuprofenate and the lowest – containing [PheOPr][IBU]. However, it should be noted that no significant difference was found between the stability parameters of the compositions tested. Furthermore, all of the tested polyacrylate compositions were decomposed in two stages.

One of the most critical properties of pressure-sensitive adhesives is their cohesion. The medical plaster should adhere well to the skin and be easily removable without adhesive residue. Table 5 shows the time needed to break the material from the steel plate. The above measurements show that good cohesive properties characterized all obtained

Table 5 Parameters characterizing obtained transdermal patches[a]

No.	Patches	T_g/°C	T_{onset}/°C	T_{max}/°C	Coat weight [g m^{-2}]	Shear strength	Adhesion [N/25 mm]	Tack [N]
1	TP	−19.80	269.3	335.3	39	>72 h	10.03	1.07
2	TP-[IBU]	−48.36	227.6	335.7	31	2 min	3.65	1.88
3	TP-[IBU][Na]	−19.47	273.3	382.6	33	172 min	0.03	0.05
4	TP-[PheOPr][IBU]	−39.75	231.7	332.7	36	16 min	5.74	0.11
5	TP-[TyrOPr][IBU]	−40.77	262.9	348.5	33	7 min	33.58	3.75
6	TP-[TrpOPr][IBU]	−14.62	264.7	345.8	49	22 min	13.28	6.13

[a] T_g – glass transitions; T_{onset} – the onset of the thermal degradation; T_{max} – maximum decomposition temperature.

polyacrylate adhesives. For patches containing active substances in their composition, the time needed to tear the material is shortened, which may be caused by a decrease in the cross-linking density of the adhesive. Moreover, the breaking time of the test patches with the addition of the active substance was compared to the time needed to break the commercial products described in the literature.[44] The data indicate that the average break time for commercially available materials was between 3 and 10 minutes, while for the materials obtained, this time was 2 to 22 minutes. The amount and nature of the added compound could influence the increase of cohesion of the obtained materials.

Adhesion determines the strength of the bond between an adhesive and the surface to which it is attached. This is an especially important aspect of the design of medical patches because it determines factors such as the formation of trauma or irritation when the medical patch is removed from the skin. The adhesion of the TP without active substance was 10.03 N, while a greater value was obtained for TP-[TyrOPr] [IBU]. The lowest adhesion value was obtained for the patch with [IBU][Na] – 0.03 N. Such a high decrease in adhesion in the case of the composition with sodium ibuprofenate was caused by the crystallization of ibuprofenate from the adhesive matrix or the difficulty in dissolving this compound during the preparation of the adhesive composition.

The tack test was also investigated, which assesses the effectiveness of transdermal patch adhesion by measuring the debonding force on applying light pressure for a short time. Table 5 shows the tack test results for the cross-linked adhesive film and the cross-linked adhesive films containing the active ingredient. The highest tack has the TP containing [TrpOPr] [IBU] (6.13 N). In turn, the lowest values were recorded for [IBU] [Na] (0.05 N).

In our *in vitro* study, the penetration of ibuprofen and amino acid propyl ester ibuprofenates from obtained patches with acrylic PSA was compared with the commercial product. Results of the *in vitro* efficiency permeation experiments related to ibuprofen are summarized in Table 6. The permeation profiles of ibuprofen from obtained transdermal patches through pigskin are shown in Fig. 9.

It was shown that the patches with the obtained acrylic PSA are an excellent alternative to the commercial ibuprofen patch.

Also, the patch with the unmodified active substance shows a worse permeation profile, similar to the commercial product. The cumulative mass of the tested compounds in acceptor fluid, considering all time points, is presented in Fig. 8. While the content of IBU and its derivatives in the acceptor fluid collected during 24 h permeation is summarized in Table 6. The cumulative mass of the individual compounds, determined after 24 h of permeation, was as follows: TP-[PheOPr][IBU] > TP-[TyrOPr] [IBU] > TP-[TrpOPr][IBU] > TP-[IBU][Na] > TP-[IBU] > commercial product. From among the studied patches, TP-[PheOPr] [IBU] permeated significantly higher than others; the cumulative amount of substance permeated during the 24 h study was 93.83 μg IBU per cm^2. However, the permeation of all derivatives differed significantly from [IBU] and the commercial preparation (Fig. 8 and S46†). These results are also confirmed by the cluster analysis test, in which TP-[PheOPr][IBU], TP-[TyrOPr] [IBU], and TP-[TrpOPr][IBU] form a separate cluster (Fig. S47†). In most cases, it was also found the similarity between derivatives and [IBU] or commercial products using the Wilcoxon test ($p < 0.05$) (Table S2†).

The steady-state flow for the investigated transdermal patches ranged from 3.14 μg cm^{-2} for the patch containing [TrpOPr][IBU] to 4.55 μg cm^{-2} for the patch containing pure ibuprofen.

The patch containing [TyrOPr][IBU] (0.0026 cm h^{-1}) was characterized by the highest obtained derivatives value of the permeation coefficient. All the obtained results had a similar value of the permeation rate to pure ibuprofen and a commercial product.

The use of ibuprofen modification in transdermal patches generally increased the delay time, where for a commercial product, this time was about 22 seconds, and for [PheOPr][IBU], this time was about 1 h.

In the case of the investigated medical patches, the product containing sodium ibuprofenate (about 3.98 cm^2 h^{-1}) was characterized by the highest diffusion coefficient, the lowest – TP-[PheOPr][IBU]. The value of the skin partition coefficient was compared for all the products obtained. The highest value of this parameter was characterized by TP-[PheOPr][IBU].

The highest percentage of the applied dose was achieved for the patch containing TP-[PheOPr][IBU] (about 3.3%) after 24 hours of testing.

Fig. 9 shows the permeation rate of L-amino acid propyl esters ibuprofenates in particular time intervals. The permeation rate of propyl ibuprofenate transdermal patches was the highest in the first hour of the study for ibuprofen and sodium

Table 6 Skin permeation parameters for ibuprofen and amino acid isopropyl ester ibuprofenates from obtained transdermal patches[a]

No.	Patches	Cumulative permeation mass, [μg]	J_{SS} [μg cm^{-2}]	$K_P \times 10^3$ [cm h^{-1}]	L_T [min]	D [cm^2 h^{-1}]	K_m	$Q\%_{24h}$
1	Commercial product	9.61	5.23	3.7	0.35	0.143	0.0013	2.0
2	TP-[IBU]	12.69	4.55	3.2	0.31	1.606	0.0001	2.7
3	TP-[IBU][Na]	40.68	3.54	2.5	0.13	3.981	0.0000	2.6
4	TP-[PheOPr][IBU]	93.83	3.32	2.3	59.97	0.008	0.0139	3.3
5	TP-[TyrOPr][IBU]	81.38	3.77	2.6	18.11	0.028	0.0048	2.7
6	TP-[TrpOPr][IBU]	75.49	3.14	2.2	43.57	0.012	0.0096	2.4

[a] J_{SS} – steady-state flux; K_P – permeability coefficient; L_T – lag time; D – diffusion coefficient; K_m – skin partition coefficient; Q – the percentage of the applied dose.

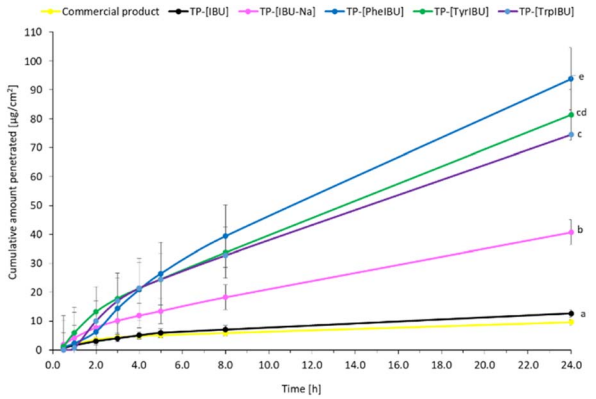

Fig. 8 Ibuprofen and amino acid propyl ester ibuprofenates permeation profiles from obtained transdermal patches. Values are the means with standard deviation; $n = 3$.

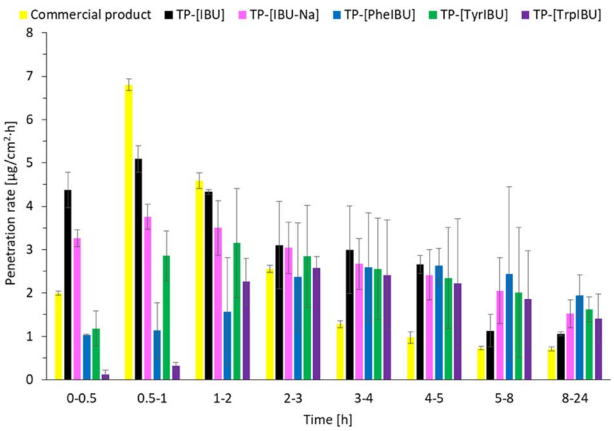

Fig. 9 The permeation rate of ibuprofen and amino acid isopropyl ester ibuprofenates during the 24 h permeation from obtained transdermal patches; $\alpha = 0.05$ (mean ± SD; $n = 3$).

ibuprofenate. In the case of L-tyrosine propyl ester ibuprofenate, the highest permeation rate was between 1 and 2 hours of the study, while for L-tryptophan propyl ester ibuprofenate, between 2 and 3 hours of the study. Propyl ester ibuprofenate L-phenylalanine achieved its highest penetration value between the 4 and 5 hours of the study.

Fig. 10 shows the mass of [IBU] and its derivatives accumulated in porcine skin after 24 h of penetration. All the compounds used accumulated in the skin. The lowest accumulation for derivatives IBU values were obtained for TP = [TyrOPr][IBU] (26.852 ± 8.325 μg IBU per g skin), while the greatest accumulation in the skin is observed for TP-[IBU] (46.043 ± 9.597 μg IBU per g skin).

Experimental

Materials

All used in this research reagents were commercially available materials and were used without further purification. (*R*,*S*)-Ibuprofen (>98%) was provided from Am-Beed (Arlington Heights, IL, USA). Thionyl chloride (99.5%) was obtained from Acros Organics (Geel, Belgium). L-Histidine (≥99%) and L-phenylalanine (>98.5%) were purchased from Carl Roth (Karlsruhe, Germany). L-Tyrosine, acetonitrile (≥99.9%) for HPLC gradient grade, deuterated DMSO (99.9%), 2-ethylhexyl acrylate (2-EHA) (98%), isobornyl methacrylate (IBOMA) (>99%), azobis(isobutyronitrile) (AIBN) (99%), and *n*-octanol (≥99%) were provided by Sigma-Aldrich (Steinheim am Albuch, Germany). L-Tryptophan was provided by Tokyo Chemical Industry Co., Ltd (TCI, Tokyo, Japan). Propanol (PrOH), ammonium hydroxide solution 25% ($NH_3 \cdot H_2O$), anhydrous sodium sulfate, *n*-hexane, methylene chloride, and diethyl ether were high-purity obtained from Chempur (Gliwice, Poland). 4-Acryloyloxy

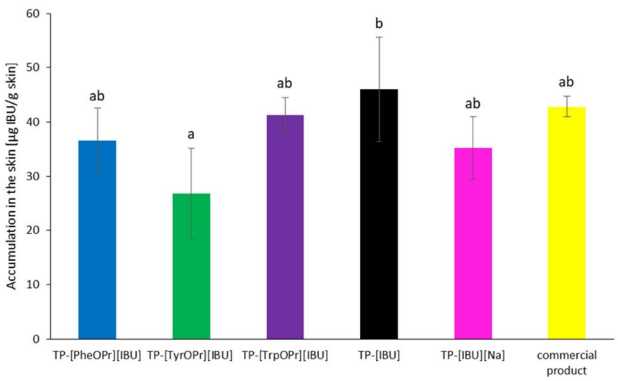

Fig. 10 Accumulation in the skin of IBU during the 24 h penetration from obtained transdermal patches.

benzophenone (ABP) was obtained from POLY-CHEM BmbH (Bitterfeld-Wolfen, Germany). Acrylic acid (AA) (>98%), ethanol (EtOH), chloroform, toluene, and ethyl acetate were of analytical grade purchased from StanLab (Lublin, Poland). Deuterated chloroform ($CDCl_3$) (99.8%) (+0.03% TMSCl) was purchased from Eurisotop (Cheshire, England).

Synthesis of the [AAOPr][IBU]

For synthesizing all obtained ibuprofen derivatives, we used the previously described three-step method,[15,33,35] which was also successfully used to obtain other salts of ibuprofen amino acid alkyl esters, ketoprofen, naproxen, and salicylic acid.[45–48] A reaction scheme for preparing amino acid propyl ester ibuprofenates is shown in Fig. 11.

In the first step, the amino acid was esterified with a chlorinating agent, which also served as the reaction catalyst, in the presence of an excess of propanol as the reaction medium. For this, thionyl chloride was used in a molar excess of 1 : 3 (AA/$SOCl_2$). However, thionyl chloride was chosen due to the weak reactivity of histidine, tyrosine, and tryptophan. Therefore, derivatives of these amino acids could not be obtained using the safer trimethylsilane chloride. During the addition of the chlorinating agent, the reaction was carried out at a temperature of about 0 °C. Then the reaction system was heated to a temperature of 60 °C. The reaction was carried out for 24–48 hours. Next, the hydrochloride was isolated from the reaction system by distillation, followed by extraction with chloroform and washing with diethyl ether. Next, hydrochloride was dried at a temperature of 60 °C under a pressure of 20 mbar for 12 h. In the second stage, the obtained hydrochloride was neutralized with a base (25% ammonia solution) to obtain amino acid alkyl esters. Diethyl ether or ethyl acetate extraction isolated the product from the reaction mixture. The solvent was then distilled from the mixture. In the final step, the obtained amino acid alkyl ester reacted with an equimolar amount of ibuprofen. The reaction was carried out in chloroform at room temperature for 30 min. After this time, the solvent was distilled off at 60 °C in a vacuum evaporator. Next, the product was dried in a vacuum oven for 24 hours at 60 °C and 20 mbar pressure.

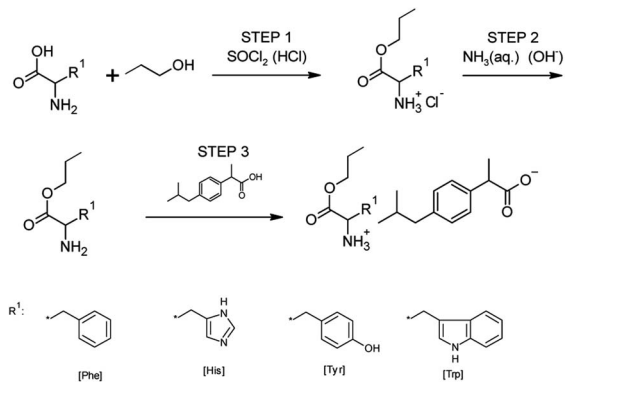

Fig. 11 Reaction scheme for the preparation of amino acid ester ibuprofenates [AAOPr][IBU].

[HisOPr][IBU] – L-histidine propyl ester bis(ibuprofenate)

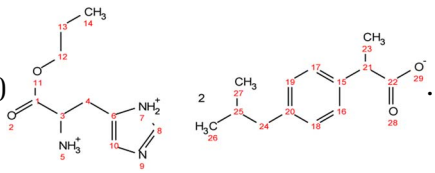

Yield: 10%. ^{1}H NMR (400 MHz, $CDCl_3$) δ in ppm: 8.35 (s, 5H, H5, H7), 7.56 (s, 1H, H8), 7.23 (d, J = 8.2 Hz, 4H, H16, H17), 7.07 (d, 4H, J = 8.0 Hz, H18, H19), 6.70 (s, 1H, H10), 4.06 (t, J = 6.7 Hz, 2H, H12), 3.76 (dd, J = 7.3, 4.5 Hz, H3), 3.68 (q, J = 7.1 Hz, 2H, H21), 3.05 (dd, J = 15.1, 4.4 Hz, 1H, H4), 2.89 (dd, J = 15.1, 7.3 Hz, 1H, H4), 2.43 (d, J = 7.1 Hz, 4H, H24), 1.86–1.79 (m, 2H, H2, H25), 1.62 (h, 2H, H13), 1.48 (d, J = 7.1 Hz, 6H, H23), 0.93 (t, J = 7.4 Hz, 3H, H14), 0.88 (d, J = 6.6 Hz, 12H, H26, H27); ^{13}C NMR (100 MHz, $CDCl_3$) δ in ppm: 179.87 (C22), 172.83 (C1), 140.30 (C15), 138.60 (C20), 134.68 (C8), 129.86 (C6), 129.26 (C16, C17), 127.29 (C18, C19), 119.15 (C10), 67.31 (C12), 53.67 (C3), 45.97 (C21), 45.05 (C24), 30.20 (C25), 28.98 (C4), 22.42 (C13), 21.89 (C18), 18.61 (C23), 10.34 (C14); ATR-FTIR: 2953, 2925, 2868, 1743, 1549, 1511, 1459, 1420, 1383, 1364, 1216, 1185, 1088, 1062, 1021, 998, 931, 881, 847, 785, 754, 727, 661, 628, 545 cm^{-1}; elemental analysis: calc. (%) for $C_{35}H_{51}N_3O_6$ (609.796): C (68.94), H (8.43), N (6.89), O (15.74), found: C (68.93), H (8.44), N (6.90), O (15.75).

[PheOPr][IBU] – L-phenylalanine propyl ester ibuprofenate

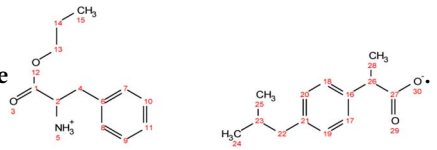

Yield: 97%. ^{1}H NMR (400 MHz, $CDCl_3$) δ in ppm: 7.29–7.20 (d, t, 5H, H9, H10, H11, H17, H18), 7.16 (d, 2H, J = 8.4 Hz, H17, H18), 7.07 (d, 2H, J = 8.1 Hz, H19, H20), 4.76 (s, 3H, H5), 4.06 (t, J = 6.7 Hz, 2H, H13), 3.80 (dd, J = 7.3, 5.5 Hz, 1H, H2), 3.67 (q, J = 7.2 Hz, 1H, H26), 3.08 (dd, J = 13.6, 5.5 Hz, 1H, H4), 2.93 (dd, J = 13.6, 7.3 Hz, 1H, H4), 2.44 (d, J = 7.2 Hz, 2H, H22), 1.79–1.89 (m, 1H, H26), 1.63 (h, 2H, H14), 1.48 (d, J = 7.1 Hz, 3H, H28), 0.90 (d, t, 9H, H15, H24, H25); ^{13}C NMR (100 MHz, $CDCl_3$) δ in ppm: 179.17 (C27), 174.47 (C1), 140.58 (C16), 137.71 (C21), 136.62 (C6), 129.33 (C7, C8, C17, C18), 128.64 (C9, C10), 127.26 (C19, C20), 126.97 (C11), 66.77 (C13), 55.17 (C2), 45.16 (C26), 45.06 (C22), 40.42 (C4), 30.20 (C23), 22.42 (C24, C25), 21.90 (C14), 18.33 (C28), 10.38 (C15); ATR-FTIR: 2953, 2922, 2867, 2638, 1750, 1732, 1620, 1510, 1457, 1382, 1363, 1328, 1310, 1289, 1263, 1228, 1170, 1062, 1022, 1010, 934, 912, 883, 853, 786, 756, 741, 728, 698, 669, 636, 595, 540, 491, 431 cm^{-1}; elemental analysis: calc. (%) for $C_{25}H_{35}NO_4$ (413.550): C (72.61), H (8.53), N (3.39), O (15.48), found: C (72.62), H (8.54), N (3.40), O (15.47).

[TyrOPr][IBU] – L-tyrosine propyl ester ibuprofenate

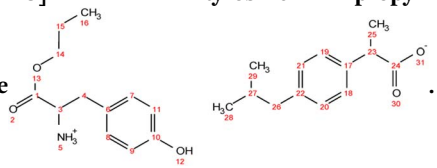

Yield: 96%. ^{1}H NMR (400 MHz, $CDCl_3$) δ in ppm: 7.23 (d, J = 8.1 Hz, 2H, H18, H19), 7.08 (d, J = 8.1 Hz, 2H, H20, H21), 6.94 (d, J =

8.4 Hz, 2H, H7, H8), 6.62 (d, J = 8.5 Hz, 2H, H9, H11), 5.50 (s, 4H, H5, H12), 4.08 (t, J = 6.7 Hz, 2H, H14), 3.76 (dd, J = 7.4, 5.1 Hz, 1H, H3), 3.68 (q, J = 7.2 Hz, 1H, H23), 3.02 (dd, J = 13.9, 5.1 Hz, 1H, H4), 2.83 (dd, J = 13.9, 7.4 Hz, 1H, H4), 2.43 (d, J = 7.1 Hz, 2H, H26), 1.88–1.77 (m, 1H, H27), 1.65 (h, J = 7.1 Hz, 2H, H15), 1.48 (d, J = 7.2 Hz, 3H, H25), 0.93 (t, J = 7.4 Hz, 3H, H16), 0.88 (d, J = 6.6 Hz, 6H, H28, H29); ^{13}C NMR (100 MHz, $CDCl_3$) δ in ppm: 179.60 (C24), 174.08 (C1), 155.44 (C10), 140.50 (C17), 137.94 (C22), 130.37 (C6), 129.31 (C7, C8), 127.27 (C18, C19), 127.19 (C20, C21), 115.77 (C9, C11), 67.03 (C14), 54.96 (C3), 45.46 (C23), 45.06 (C26), 38.95 (C4), 30.20 (C27), 22.42 (C28, C29), 21.90 (C15), 18.39 (C25), 10.38 (C16); ATR-FTIR: 2955, 2928, 2868, 1738, 1614, 1594, 1552, 1513, 1457, 1383, 1309, 1225, 1172, 1105, 1060, 1021, 1000, 928, 884, 843, 823, 800, 784, 753, 728, 679, 635, 553, 521, 434 cm^{-1}; elemental analysis: calc. (%) for $C_{25}H_{35}NO_5$ (429.549): C (69.90), H (8.21), N (3.26), O (18.62), found: C (69.91), H (8.22), N (3.26), O (18.63).

[TrpOPr][IBU] – L-tryptophan propyl ester ibuprofenate

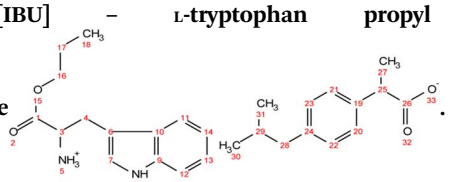

. Yield: 96%. ^{1}H NMR (400 MHz, $CDCl_3$) δ in ppm: 8.22 (s, 1H, H5), 7.55 (d, J = 7.8 Hz, 1H, H12), 7.31 (d, J = 8.1, 0.9 Hz, 1H, H11), 7.23 (d, J = 7.8 Hz, 2H, H20, H21), 7.17 (td, J = 8.1, 1.2 Hz, 1H, H13), 7.09 (t, d, 3H, H14, H22, H23), 6.97 (d, J = 2.2 Hz, 1H, H20, H7), 5.48 (s, 3H, H22, H5), 4.03 (td, J = 6.7, 3.3 Hz, 2H, H16), 3.84 (dd, J = 7.3, 4.8 Hz, 1H, H3), 3.64 (q, 1H, H25), 3.26 (dd, J = 14.2, 5.3 Hz, 1H, H4), 3.08 (dd, J = 14.6, 7.3 Hz, 1H, H4), 2.43 (d, J = 7.2 Hz, 2H, H28), 1.87–1.78 (m, 1H, H29), 1.60 (h, J = 7.1 Hz, 2H, H17), 1.46 (dd, J = 7.2, 1.6 Hz, 3H, H27), 0.92–0.83 (d, t, 9H, H18, H30, H31); ^{13}C NMR (100 MHz, $CDCl_3$) δ in ppm: 179.14 (C26), 174.25 (C1), 140.42 (C19), 138.27 (C24), 136.26 (C9), 129.30 (C20, C21), 127.36 (C10), 127.31 (C22, C23), 123.40 (C7), 122.17 (C13), 119.54 (C14), 118.62 (C11), 111.29 (C12), 110.07 (C6), 66.91 (C16), 54.11 (C3), 45.52 (C25), 45.07 (C28), 30.22 (C29), 29.61 (C4), 22.43 (C31, C30), 21.88 (C17), 18.46 (C27), 10.35 (C18); ATR-FTIR: 2955, 2926, 2868, 1737, 1549, 1511, 1457, 1420, 1383, 1357, 1282, 1215, 1092, 1061, 1009, 929, 882, 850, 796, 739, 667, 548, 461, 426 cm^{-1}; elemental analysis: calc. (%) for $C_{27}H_{36}N_2O_4$ (452.586): C (71.65), H (8.02), N (6.19), O (14.14), found: C (71.66), H (8.02), N (6.18), O (14.14).

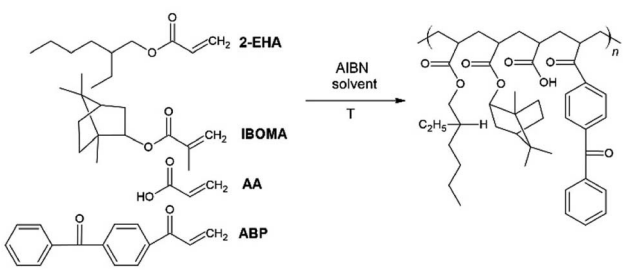

Fig. 12 The schematic representation of the acrylic copolymer synthesis.

Synthesis of the acrylic PSA

The acrylic PSA was synthesized in ethyl acetate (50 wt% polymer content) from 70–80 wt% 2-ethylhexyl acrylates – 2-EHA, 25 wt% of monomer increasing T_g (hard) – IBOMA, 5 wt% of monomers containing functional groups – acrylic acid – AA, and 0.5 wt% of unsaturated copolymerizable acryloyloxyphotoinitiator – ABP (Fig. 12). The polymerization process was carried out under the following conditions: 2 h dosage time of monomers mixture and 5 h post-reaction time in the presence of 0.1 wt% radical starter azobisisobutyronitrile (AIBN) at the temperature of 78 °C (boiling point of ethyl acetate). The reaction was carried out until the bands characteristic for acrylate groups disappeared – sharp peaks at 1636, 1409, and 809 cm^{-1} (ATR-FTIR control). This confirms that the copolymerization reaction has taken place and obtaining copolymers with complete conversion of acrylate groups. Moreover, a new peak at 1160 cm^{-1} is observed in the spectrum after the synthesis, probably responsible for forming ester bonds. The obtained acrylate copolymer was characterized in terms of solid weight content determined *via* gravimetry, which was approximately 80%, as well as viscosity and glass transition temperature, which were respectively η = 0.72 Pa s and T_g = −19.8 °C.

Preparation of transdermal patches

Obtained acrylate copolymers constituted the adhesive matrix of the transdermal patches. Adhesive films with and without active substances were obtained. Ibuprofen, sodium ibuprofenate and ibuprofenates of L-phenylalanine, L-tyrosine and L-tryptophan propyl esters were used as active substances. For this purpose, adhesives with or without API were coated (250 μm) on a polyester film. The weight ratio of the adhesive matrix to active substance was calculated based on the adhesive characteristics, *i.e.*, solids content, the basis weight depends on the applied thickness of the adhesive film, the characteristics of the active substance, the molar mass, and the initial assumption regarding the content of active substances in commercial products – 200 mg of active substance for the surface of the adhesive film equal to 140 cm^2. The adhesive compositions were prepared by dissolving the active substance in ethyl acetate and then adding the mixture to the adhesive matrix. This step was omitted in the case of the patch without the addition of an active substance. In the next stage, the obtained adhesives were cross-linked after 10 min at 110 °C with a transfer UV lamp (Aktiprint drying-mini-18-2; UV dose: 12 × 650 mJ cm^{-2}). The resulting adhesive film layer was covered with siliconized release paper.

General analytical methods

Nuclear magnetic resonance spectroscopy (NMR). NMR spectra were made on a BRUKER DPX-400 spectrometer (Billerica, MA, USA) at 400 MHz for ^{1}H NMR spectra and 100 MHz for ^{13}C NMR spectra. $CDCl_3$ or DMSO-d_6 was used depending on the solubility of obtained compounds.

Total reflectance – Fourier transform infrared spectroscopy (ATR-FTIR). The FTIR spectra were made using a Nicolet iS5 IR

spectrometer from Thermo Electron Corporation (Waltham, MA, USA). The study used the ATR attachment with a diamond crystal. The measurement range was from 4000–400 cm^{-1} at a resolution of 4 cm^{-1}. The analysis was performed with the use of Omnic version 7.3.

Elemental analysis. The elemental composition was determined on Thermo Scientific™ FLASH 2000 CHNS/O Analyzer (Waltham, MA, USA). 2,5-Bis(5-*tert*-butyl-2-benzo-oxazol-2-yl) thiophene, L-cysteine, L-methionine, and sulphanilamide were used as standards in CHNS-mode and acetanilide, and benzoic acid were used for calibration in O-mode respectively. The samples were prepared in the tin (CHNS analysis) or silver (O analysis) crucibles and were weighed with an accuracy of ±0.000001 *g*.

Thermogravimetric analysis. The thermal stability was determined using the Netzsch Proteus Thermal Analysis TG 209 F1 Libra thermobalance (Selb, Germany) in the temperature range of 25–1000 °C under nitrogen (flow 10 ml min^{-1}) and air (25 ml min^{-1}). The weight of the samples was approximately 5 mg.

Differential scanning calorimetry (DSC). Phase transition temperatures of the obtained compounds and medical patches were made using the DSC Q-100 differential scanning calorimeter from TA Instruments (New Castle, DE, USA). The tests were carried out in the range from 25 °C to the temperature of the onset of decomposition of the compound, determined using TG (for compounds). Or in the range of −90 °C to +100 °C for medical patches. The samples weighing about 10 mg were analyzed in closed aluminum crucibles. The rate of heating/cooling/heating was 10°C min^{-1}. Indium and mercury were used as standards to calibrate the temperature. Heat calibration used indium.

Melting point. The melting points of the compounds obtained were determined with an OptiMelt MPA 100 apparatus (SRS – Stanford Research System, Sunnyvale, CA, USA). The measurement parameters were as follows: range 25–350 °C, heating rate 5 °C min^{-1}, and measurement accuracy of 0.3 °C.

Specific rotation. Optical rotation was analyzed using an Autopol IV polarimeter from Rudolph Research Analytical (Hackettstown, NJ, USA) at 589 nm and a temperature of 25 °C. Solutions of the analyzed compounds in anhydrous ethanol were prepared for the tests. The concentration of the compounds was about 1%. The angular rotation was determined at the accuracy of 0.001° at 20 ± 0.1 °C. The specific rotation was determined using eqn (1), and the molar one using eqn (2):

$$[\alpha]_\lambda^T = \frac{\alpha_\lambda^T}{cl} \quad (1)$$

$$[M]_\lambda^T = \frac{M[\alpha]_\lambda^T}{100} \quad (2)$$

where: α_λ^T – optical rotation at temperature T and wavelength λ [° Arc], $[\alpha]_\lambda^T$ – specific rotation at temperature T and wavelength λ, c – concentration [g cm^{-3}], l – cell length [dm], M – the molar mass of the tested substance [g mol^{-1}].

XRD. The test was performed using the Aeris XRays ON X-ray diffractometer by Malvern Panalytical Ltd (Malvern, United Kingdom). The crystallinity degree of the compounds prepared by the X-ray powder diffraction method was determined. The tests were carried out in the range of 7–90° 2θ, using Cu-Kα radiation (λ = 1.54056 Å).

Solubility in water and organic solvents. The solubility of the synthesized compounds was tested using the Vogel method.[42] Vials with a capacity of 4 ml were prepared, into which about 10 mg of the tested compounds were weighed. Then, water, ethanol, chloroform, dimethylsulfoxide, *n*-hexane, methylene chloride, diethyl ether, and ethyl acetate were added to each vial. The solubility was classified as good when the compound dissolved in 100 μl of the solvent and difficult when the test compound dissolved in 100 μl to 300 μl. The insoluble substance in 300 μl of the selected solvent was considered insoluble.

Solubility in water solution. The solubility of the synthesized compounds was tested for saturated aqueous solutions. 2 ml of water was added to about 15 mg of the compound. The resulting solutions were then stirred for 24 h at 25 °C. After the allotted time, the heterogeneous solutions were filtered through a syringe filter, and the concentration of the saturated solutions was determined by high-performance liquid chromatography. The measurements were carried out on the SHIMADZU Nexera-i LC-2040C 3D High Plus Liquid Chromatograph HPLC (Kyoto, Japan). The chromatograph was equipped with a DAD/FLD detector and a Kinetex F5 100 Å column with a porosity of 2.6 μm, dimensions 150 × 4.6 mm, from Phenomenex (Torrance, CA, USA). The mobile phase was a 50 : 50 mixture of water and acetonitrile with a flow – 1 ml min^{-1}. The samples were placed in an autosampler thermostated to a temperature of 25 °C. Injections were repeated at least three times for each sample, and the results were averaged. Chromatograms recorded at a wavelength of 210 nm were used for the analysis. The calibration curve method calculated the ibuprofenate concentration from peak area measurements.

Partition coefficient. The *n*-octanol/water partition coefficient was determined using the shake flask method. For this, 5 ml of water saturated with *n*-octanol and 5 ml of *n*-octanol saturated with water were added to 10 mg of the compound. The solution was stirred on a magnetic stirrer at 25 °C for 3 h. After the allotted time, the layers were separated. The concentration of ibuprofenates in the aqueous layer was determined using the HPLC method, analogous to the dissolution test.

Based on the difference in concentrations, the concentration of substances in the *n*-octanol layer was determined according to eqn (3):

$$C_{out} = C_0 - C_w \text{ mg dm}^{-3} \quad (3)$$

where: C_{oct} – concentration of the substance in the organic (*n*-octanol) layer [mg dm^{-3}], C_0 – total concentration calculated based on the mass of the compound used in the study [mg dm^{-3}], C_w – concentration of the substance in the water layer [mg dm^{-3}].

Lipophilicity ($\log P$) is quantified using the partition coefficient P or $\log P$ calculated according to eqn (4):

$$\log P = \log C_0 - \log C_w \quad (4)$$

The permeability of the active substance through the skin. The research was carried out using the Franz diffusion cells Phoenix DB-6 model by Teledyne Hanson Research (Thousand Oaks, CA, USA). The acceptor chamber with a volume of 8 cm^3 was a PBS solution (pH 7.4), temperature 37.0 ± 0.5 °C. The acceptor chamber contents were mixed with a magnetic stirrer at a constant speed for all chambers (400 rpm).

In the donor chamber, 1 cm^3 of about 5% of a solution of the test compounds in 70% ethanol was placed (concentration of about 0.05 g cm^{-3}). The donor chamber was covered with a stopper to prevent possible evaporation of the test solution. Pig skin (abdominal flap) was used for the study as it has a similar permeability to human skin.[42] The analysis was carried out for 24 hours.

Samples were taken after 0.5 h, 1 h, 2 h, 3 h, 4 h, 5 h, 8 h and 24 h of mixing, respectively. After the appointed time, portions of the tested acceptor fluid were withdrawn in the amount of 0.3 cm^3, and the acceptor chamber was refilled with the buffer (with the same pH). The concentrations of compounds in the acceptor fluid were determined using high-performance liquid chromatography (HPLC).

An analogous experiment was also carried out using the tested active substances' manufactured patches. For this purpose, the patches were cut to 1 cm^2 and then glued to the pig skin to cover its entire surface. The experiment, as in the case of the analysis of solutions, was performed for 24 hours. Samples of the acceptor fluid were collected after 0.5 h, 1 h, 2 h, 3 h, 4 h, 5 h, 8 h and 24 h of mixing. After the appointed time, 0.3 cm^3 portions of the tested acceptor fluid were taken, and the acceptor chamber was refilled with buffer (same pH). The concentrations of the obtained ibuprofenates in the acceptor fluid were measured using high-performance liquid chromatography (HPLC).

The permeability parameters were calculated according to the methodology presented in the literature.

From the curves of the dependence of the cumulative mass of compounds on time, the steady-state flow (J_{ss}) estimated from the slope of the linear curve of the plot of the cumulative mass in the acceptor phase over time was determined and the time needed to reach the steady state permeation (L_T), selected from the point of intersection of the plot of the function with the x-axis. Eqn (5) was used for the calculations:

$$A = J_{ss} \times (t - L_T) \quad (5)$$

where: A – cumulative amount of ibuprofenates penetrating the acceptor fluid [μg cm^{-2}], J_{ss} – steady-state flux [μg cm^2 h^{-1}], t – time [h], L_T – lag time [h].

The permeability coefficient (K_p) was calculated according to eqn (6):

$$K_p = \frac{J_{ss}}{C} \quad (6)$$

where: C – concentration of the substance in the donor phase.

The diffusion coefficient (D) was also determined based on eqn (7):

$$D = \frac{h^2}{6} \times L_T \quad (7)$$

where: h – skin thickness [mm].

The skin partition coefficient was calculated using eqn (8):

$$K_m = K_p \times \frac{h}{D} \quad (8)$$

Accumulation in the skin. The accumulation of API in the skin after penetration was determined using previously described methods.[33,35,44,49] For this purpose, after 24 h penetration test, skin samples were removed from the Franz diffusion cell. The skin samples were carefully rinsed in PBS solution at 7.4 pH and dried at room temperature. Next, skin samples were weighed, cut by the diffusion area (1 cm^2), and minced using scissors. Afterward, the skin was placed in 2 cm^3 methanol and incubated for 24 h at 4 °C. After this time, skin samples were homogenized for 3 min using a homogenizer (IKA®T18 digital ULTRA TURRAX (Staufen im Breisgau, Germany)). The homogenate was centrifuged at 3500 rpm for 5 min. The supernatant was collected and analyzed by the HPLC method. In addition, a liquid chromatography system (Knauer, Berlin, Germany) assessed the concentration of IBU and its derivatives in the acceptor fluid in permeation and release tests and accumulation in the skin.

Viscosity. The viscosity of the obtained acrylate copolymers was determined with a Bohlin Vis-co 88 (Malvern Panalytical) viscometer. The measurement was carried out at a temperature of 20 °C using the C14 geometry at a speed of 20 rpm.

Solid weight content. Solid weight content was determined by ISO 3251 (140 °C, 30 min) using a moisture analyzer (Radwag MAX 60/NP).

Coat weight. The coat weight of the cross-linked adhesive films (after evaporation of the solvent and after UV irradiation) was measured with a circular punch 1009 with an area of 10 cm^2 (Karl Schröder KG, Germany).

Cohesion. The shear strength test of the obtained adhesive tapes was tested in accordance with FINAT FTM 8 at room temperature.[33,50]

Adhesion. The peel adhesion measurement was performed on the Zwick/Roell Z010 testing machine according to AFERA 4001 at room temperature.[33,50]

Tack. The tack measurements for the obtained patches were tested per the AFERA 4015 standard using the Zwick/Roell Z010 testing machine.[33,50,51]

Statistical analysis. Results are presented as the mean ± standard deviation (SD). A one-way analysis of variance (ANOVA) was used. In the case of the cumulative mass, the significance of differences between individual groups was evaluated with Tukey's test ($\alpha < 0.05$). A cluster analysis was carried out to determine similarities between all compounds tested,

considering all time points. On this basis, presented groups of compounds with a similar permeation. Significant differences in the cumulative mass between all analyzed compounds, taking into account all time points during the entire 24 h permeation, were also estimated by the Wilcoxon test. Statistical calculations were done using Statistica 13 PL software (StatSoft, Kraków, Polska).

Conclusions

As part of the presented research, amino acid propyl ester ibuprofenates were synthesized, identified, and characterized. It was shown that the obtained structural modifications of ibuprofen show higher water solubility and lower lipophilicity than ibuprofen. The obtained derivatives have also been successfully used as active substances in transdermal patches based on biocomponents. Work is a comprehensive approach to increasing the permeability of active substances through the skin.

Author contributions

Conceptualization, P. O.-R.; methodology, P. O.-R., P. B. and A. N.; formal analysis, P. O.-R., K. S., M. N., A. N., W. D., Ł. K., Ł. S. and Z. C.; investigation, P. O.-R.; writing – original draft preparation, P. O.-R.; writing – review and editing, P. O.-R.; visualization, P. O.-R.; supervision, P. O.-R.; A. K. and Z. C.; project administration, P. O.-R.; funding acquisition, P. O.-R. All authors have read and agreed to the published version of the manuscript.

Conflicts of interest

There are no conflicts to declare.

Acknowledgements

This study was supported by the National Centre for Research and Development (grant number LIDER/53/0225/L-11/19/NCBR/2020).

References

1 M. Merskey, D. Albe Fessard, J. J. Bonica, A. Carmon, R. Dubner, F. W. L. Kerr, U. Lindblom, J. M. Mumford, P. W. Nathan, W. Noordenbos, C. A. Pagni, M. J. Renaer, R. A. Sternbach and S. Sunderland, *Pain*, 1979, **6**, 249.
2 S. N. Raja, D. B. Carr, M. Cohen, N. B. Finnerup, H. Flor, S. Gibson, F. J. Keefe, J. S. Mogil, M. Ringkamp, K. A. Sluka, X.-J. Song, B. Stevens, M. D. Sullivan, P. R. Tutelman, T. Ushida and K. Vader, *Pain*, 2020, **161**, 1976–1982.
3 M. Cohen, J. Quintner and S. van Rysewyk, *Pain Rep.*, 2018, **3**, e634.
4 I. Jordan, R. Martens and K. A. Birnie, *Pediatr. Neonatol. Pain*, 2021, **3**, 119–122.
5 A. A. Anekar and M. Cascella, *StatPearls*, StatPearls Publishing, Treasure Island (FL), 2022.
6 B. J. Walker, D. M. Polaner and C. B. Berde, *A Practice of Anesthesia for Infants and Children*, Elsevier, 2019, pp. 1023–1062.
7 P. Ossowicz-Rupniewska, R. Rakoczy, A. Nowak, M. Konopacki, J. Klebeko, E. Świątek, E. Janus, W. Duchnik, K. Wenelska, Ł. Kucharski and A. Klimowicz, *Int. J. Mol. Sci.*, 2021, **22**, 6252.
8 F. Cilurzo, P. Minghetti, A. Casiraghi, L. Tosi, S. Pagani and L. Montanari, *Eur. J. Pharm. Biopharm.*, 2005, **60**, 61–66.
9 P. K. Bolla, B. A. Clark, A. Juluri, H. S. Cheruvu and J. Renukuntla, *Pharmaceutics*, 2020, **12**, 1–19.
10 P. L. Lam and R. Gambari, *J. Controlled Release*, 2014, **178**, 25–45.
11 A. Haq and B. Michniak-Kohn, *Drug Delivery*, 2018, **25**, 1943–1949.
12 B. Balázs, G. Vizserálek, S. Berkó, M. Budai-Szűcs, A. Kelemen, B. Sinkó, K. Takács-Novák, P. Szabó-Révész and E. Csányi, *J. Pharm. Sci.*, 2016, **105**, 1134–1140.
13 H. Chen, X. Chang, D. Du, J. Li, H. Xu and X. Yang, *Int. J. Pharm.*, 2006, **315**, 52–58.
14 P. Ossowicz-Rupniewska, A. Nowak, J. Klebeko, E. Janus, W. Duchnik, U. Adamiak-Giera, Ł. Kucharski, P. Prowans, J. Petriczko, N. Czapla, P. Bargiel, M. Markowska and A. Klimowicz, *Materials*, 2021, **14**, 6808.
15 P. Ossowicz, J. Klebeko, E. Janus, A. Nowak, W. Duchnik, Ł. Kucharski and A. Klimowicz, *RSC Adv.*, 2020, **10**, 41727–41740.
16 K. A. Levis, M. E. Lane and O. I. Corrigan, *Int. J. Pharm.*, 2003, **253**, 49–59.
17 H. Potthast, J. B. Dressman, H. E. Junginger, K. K. Midha, H. Oeser, V. P. Shah, H. Vogelpoel and D. M. Barends, *J. Pharm. Sci.*, 2005, **94**, 2121–2131.
18 L. R. Shaw, W. J. Irwin, T. J. Grattan and B. R. Conway, *Drug Dev. Ind. Pharm.*, 2005, **31**, 515–525.
19 R. M. Watkinson, C. Herkenne, R. H. Guy, J. Hadgraft, G. Oliveira and M. E. Lane, *Skin Pharmacol. Physiol.*, 2009, **22**, 15–21.
20 P. Bustamante, M. A. Peña and J. Barra, *Int. J. Pharm.*, 2000, **194**, 117–124.
21 P. Schleier, A. Prochnau, A. M. Schmidt-Westhausen, H. Peters, J. Becker, T. Latz, J. Jackowski, E. U. Peters, G. E. Romanos, B. Zahn, J. Lüdemann, J. Maares and B. Petersen, *Int. J. Clin. Pharmacol. Ther.*, 2007, **45**, 89–97.
22 P. M. Dewland, S. Reader and P. Berry, *BMC Clin. Pharmacol.*, 2009, **9**, 19.
23 S. E. Nørholt, F. Hallmer, J. Hartlev, L. Pallesen, J. Blomlöf, E. J. Hansen, N. Fernandes, L. Eriksson and E. M. Pinholt, *Int. J. Clin. Pharmacol. Ther.*, 2011, **49**, 722–729.
24 P. Brain, R. Leyva, G. Doyle and D. Kellstein, *Clin. J. Pain*, 2015, **31**, 444–450.
25 M. M. Santos, L. R. Raposo, G. V. S. M. Carrera, A. Costa, M. Dionísio, P. V. Baptista, A. R. Fernandes and L. C. Branco, *ChemMedChem*, 2019, **14**, 907–911.
26 T. Lee and Y. W. Wang, *Drug Dev. Ind. Pharm.*, 2009, **35**, 555–567.

27 H. Alghurabi, *Kerbala J. Pharm. Sci.*, 2017, 337–347.
28 R. Cristofoletti and J. B. Dressman, *J. Pharm. Sci.*, 2017, **106**, 92–99.
29 R. Forbes, *Int. J. Pharm.*, 1995, **126**, 199–208.
30 S. Li, P. Doyle, S. Metz, A. E. Royce and A. T. M. Serajuddin, *J. Pharm. Sci.*, 2005, **94**, 2224–2231.
31 B. Ahmetaj-Shala, A. Tesfai, C. Constantinou, R. Leszczynski, M. V. Chan, H. Gashaw, G. Galaris, S. Mazi, T. D. Warner, N. S. Kirkby and J. A. Mitchell, *Biochem. Biophys. Res. Commun.*, 2017, **484**, 762–766.
32 J. Klebeko, P. Ossowicz-Rupniewska, A. Nowak, E. Janus, W. Duchnik, U. Adamiak-Giera, Ł. Kucharski, P. Prowans, J. Petriczko, N. Czapla, P. Bargiel, M. Markowska and A. Klimowicz, *Materials*, 2021, **14**, 6678.
33 P. Ossowicz-Rupniewska, J. Klebeko, E. Świątek, K. Bilska, A. Nowak, W. Duchnik, Ł. Kucharski, Ł. Struk, K. Wenelska, A. Klimowicz and E. Janus, *Int. J. Mol. Sci.*, 2022, **23**, 4158.
34 S. Furukawa, G. Hattori, S. Sakai and N. Kamiya, *RSC Adv.*, 2016, **6**, 87753–87755.
35 E. Janus, P. Ossowicz, J. Klebeko, A. Nowak, W. Duchnik, Ł. Kucharski and A. Klimowicz, *RSC Adv.*, 2020, **10**, 7570–7584.
36 P. Ossowicz-Rupniewska, J. Klebeko, E. Świątek, J. Szachnowska, E. Janus, M. Rangelov, N. Todorova, S. G. Taneva, E. Krachmarova and M. Guncheva, *J. Mol. Liq.*, 2022, **360**, 119367.
37 P. Ossowicz, E. Janus, G. Schroeder and Z. Rozwadowski, *Molecules*, 2013, **18**, 4986–5004.
38 R. Radeglia, *J. Prakt. Chem.*, 1981, **323**, 1015–1016.
39 Z. Rozwadowski, *J. Mol. Struct.*, 2005, **753**, 127–131.
40 S. Vairam, T. Premkumar and S. Govindarajan, *J. Therm. Anal. Calorim.*, 2010, **100**, 955–960.
41 C. Reichardt, *Solvents and solvent effects in organic chemistry*, Wiley-VCH, Weinheim, 3rd edn, 2003.
42 B. S. Furniss and A. I. Vogel, *Vogel's textbook of practical organic chemistry*, Pearson/Prentice Hall, Harlow, 5th edn, 2009.
43 S. K. Singh and A. W. Savoy, *J. Mol. Liq.*, 2020, **297**, 112038.
44 P. Ossowicz-Rupniewska, P. Bednarczyk, M. Nowak, A. Nowak, W. Duchnik, Ł. Kucharski, J. Rokicka, A. Klimowicz and Z. Czech, *Int. J. Mol. Sci.*, 2021, **22**, 11840.
45 P. Ossowicz, P. Kardaleva, M. Guncheva, J. Klebeko, E. Świątek, E. Janus, D. Yancheva and I. Angelov, *Molecules*, 2020, **25**, 90.
46 P. Ossowicz, E. Janus, J. Klebeko, E. Świątek, P. Kardaleva, S. Taneva, E. Krachmarova, M. Rangelov, N. Todorova and M. Guncheva, *J. Mol. Liq.*, 2020, **319**, 114283.
47 J. Klebeko, P. Ossowicz-Rupniewska, E. Świątek, J. Szachnowska, E. Janus, S. G. Taneva, E. Krachmarova and M. Guncheva, *Molecules*, 2021, **27**, 216.
48 P. Kardaleva, M. Guncheva, S. Todinova, I. Angelov, P. Ossowicz and E. Janus, *J. Therm. Anal. Calorim.*, 2020, **142**, 1911–1917.
49 A. Haq, B. Goodyear, D. Ameen, V. Joshi and B. Michniak-Kohn, *Int. J. Pharm.*, 2018, **547**, 432–437.
50 P. Bednarczyk, K. Mozelewska and Z. Czech, *Int. J. Adhes. Adhes.*, 2020, **102**, 102652.
51 A. Antosik, *Chem. Rev.*, 2016, **1**, 73–75.